

Improved Final Focus Shielding Designs for Modern Heavy-Ion Fusion Power Plant Designs

J.F. Latkowski and W.R. Meier

This article was submitted to
13th International Symposium on Heavy Ion Inertial Fusion,
March 13-17, 2000, San Diego, CA

U.S. Department of Energy

Lawrence
Livermore
National
Laboratory

March 2000

DISCLAIMER

This document was prepared as an account of work sponsored by an agency of the United States Government. Neither the United States Government nor the University of California nor any of their employees, makes any warranty, express or implied, or assumes any legal liability or responsibility for the accuracy, completeness, or usefulness of any information, apparatus, product, or process disclosed, or represents that its use would not infringe privately owned rights. Reference herein to any specific commercial product, process, or service by trade name, trademark, manufacturer, or otherwise, does not necessarily constitute or imply its endorsement, recommendation, or favoring by the United States Government or the University of California. The views and opinions of authors expressed herein do not necessarily state or reflect those of the United States Government or the University of California, and shall not be used for advertising or product endorsement purposes.

This is a preprint of a paper intended for publication in a journal or proceedings. Since changes may be made before publication, this preprint is made available with the understanding that it will not be cited or reproduced without the permission of the author.

This report has been reproduced
directly from the best available copy.

Available to DOE and DOE contractors from the
Office of Scientific and Technical Information
P.O. Box 62, Oak Ridge, TN 37831
Prices available from (423) 576-8401
<http://apollo.osti.gov/bridge/>

Available to the public from the
National Technical Information Service
U.S. Department of Commerce
5285 Port Royal Rd.,
Springfield, VA 22161
<http://www.ntis.gov/>

OR

Lawrence Livermore National Laboratory
Technical Information Department's Digital Library
<http://www.llnl.gov/tid/Library.html>

Improved Final Focus Shielding Designs for Modern Heavy-Ion Fusion Power Plant Designs

J. F. Latkowski* and W. R. Meier

Lawrence Livermore National Laboratory, P.O. Box 808, Mailstop L-446, Livermore, California 94550 USA

Received XXXX 2000; accepted XXXX 2000

Abstract

Recent work in heavy-ion fusion accelerators and final focusing systems shows a trend towards less current per beam, and thus, a significantly greater number of beams. Final focusing magnets are susceptible to nuclear heating, radiation damage, and neutron activation. The trend towards more beams, however, means that there can be less shielding for each magnet. Excessive levels of nuclear heating may lead to magnet quench or an intolerable recirculating power for magnet cooling. High levels of radiation damage may result in short magnet lifetimes and low reliability. Finally, neutron activation of the magnet components may lead to difficulties in maintenance, recycling, and waste disposal. The present work expands upon previous, three-dimensional magnet shielding calculations for a modified version of the HYLIFE-II IFE power plant design. We present key magnet results as a function of the number of beams.

Keywords: Inertial fusion energy; Magnet shielding; Final focus

1. Introduction

Final focusing magnets for heavy-ion fusion power plant designs must survive exposure to intense fluxes of neutrons and γ -rays. If not shielded sufficiently, superconducting final focusing magnets may be subject to quench. Normal and superconducting magnets will need to be cooled and have a high resistance to radiation damage. Finally, neutron activation and waste management may be a significant issue for some coil materials.

Previous power plant designs have been able to effectively shield the final focusing magnets due to the small number of beams (12-20) that allowed large shielding thicknesses (30-40 cm) for each magnet [1,2]. More recent work, however, has reduced the current per beam at a cost of a greater number of beams and less space per beam for magnet shielding [3,4]. Here, we utilize a self-consistent, integrated source-to-target model for induction linear accelerator (linac) drivers that includes the key interdependencies of the major subsystems in terms of cost, performance, and constraints. We

use this model to study the trade-offs between magnet shielding and the number of beams for a modified version of the HYLIFE-II power plant design [5].

2. Description of IBEAM model

The IBEAM (Ion Beams for Energy Applications Model) model has been used to establish parameters for four point design final focusing arrays. Each case assumes target illumination from two arrays of 6×6 , 8×8 , 10×10 , or 12×12 beams. The model begins with calculation of the beam spot size on target, r_s , which is calculated as:

$$r_s = \sqrt{r_{se}^2 + r_{ca}^2 + r_{ga}^2 + r_{aim}^2} \quad (1)$$

Where spot size radius contributions are:

r_{se} = coupled space charge and emittance effects
 r_{ca} = chromatic aberrations
 r_{ga} = geometric aberrations
 r_{aim} = aiming

* Corresponding author.

E-mail address: latkowski1@llnl.gov

The driver considered here is required to deliver 3.3 MJ to the target with an average spot size on target of 1.7 mm. This total beam energy can be divided into any number of beams, with economics considerations favoring a rather large number of beams (> 100 depending on the ion used) [6]. The example used in this study was for cesium ions ($A = 133$). The space charge and emittance term is found by solving the beam envelop equation for the spot size consistent with the focus half angle, q . The normalized emittance that enters the equation depends on the emittance of the source (which decreases with increasing number of beam) and how that emittance grows between the source and final focus system. We assume a total growth factor of seven, but this is the subject of ongoing research in the heavy ion fusion program. Space charge also decreases with increasing number of beams as the total required charge is divided into a larger number of beams. Space charge effects are further diminished by neutralizing the beams by 99% as they leave the final focus magnets. The chromatic aberration contribution is proportion to the momentum spread (which is held constant here), the final focus length, L_f (also constant at 5.5 m), and the final focus half angle, q , which is one of the design variables we consider. Geometric aberrations go as $(L_f q)^3$, and aiming is assumed to be a constant 200 mm. Figure 1 shows the contribution to spot size as a function of q for a 72-beam case.

To investigate the effect of smaller beam port sizes, we examined a range of cases with larger numbers of beams. In each case, the focus half angle yielding the minimum spot size on target was used to calculate the beam port size. Key parameters for the cases considered are given in Table 1. The maximum beam radius is ~ 1.3 times the average beam radius, which is simply $L_f \times q$. The bore inner radius is 1.25 times the maximum beam radius plus a 0.5 cm additional clearance allowance. The winding inner radius is at R_{bore} plus 7 cm 2 cm for the beam tube wall, insulation and cooling combined plus 5 cm for shielding. The winding thickness depends on the B-field as does the thickness of the steel collar. Windings are assumed to be constructed from 40% Nb-Ti superconductor, 40% Cu, and 20% liquid helium, on a volumetric basis.

3. Transport models

The radial builds specified in Table 1 have been used in neutron and γ -ray transport models.

These calculations yield particle spectra and energy deposition in each region of each magnet. With this information, power loadings, cooling power, radiation damage, and neutron activation may be calculated.

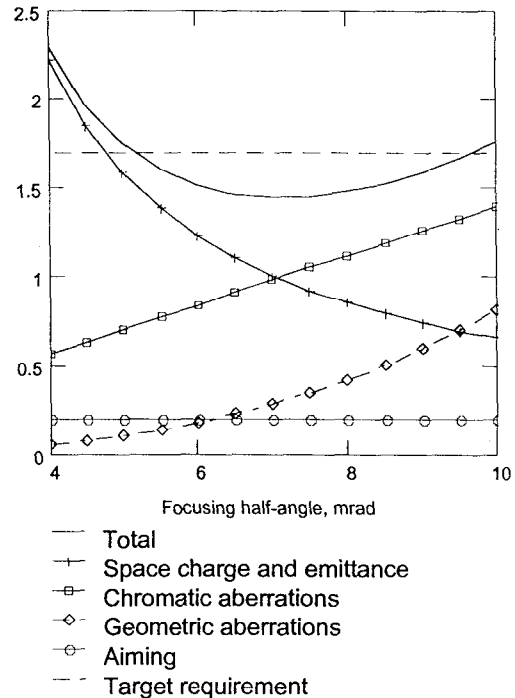


Fig. 1. Spot size vs. focus half angle for Cs^+ , 72-beam case.

Table 1
Key parameters for final focusing magnets

Parameter	Number of beams			
	72	128	200	288
θ , mrad	7	5	4	3
Beam radius (max), cm	5.0	3.6	2.9	2.1
Bore radius, cm	6.8	5.0	4.1	3.2
Winding radius, cm	13.8	12.0	11.1	10.2
Banding radius, cm	14.4	12.5	11.6	10.7
Quad outer radius	15.1	13.0	11.9	11.0
Quad field, T	3.4	3.1	2.8	2.9
Field gradient, T/m	24.6	25.6	25.6	28.4
Array half-angle at target	11.0	13.2	15.4	17.3

HYLIFE-II includes a 60-cm-thick Flibe pocket and an additional 50 cm of Flibe within the blanket [6]. The first wall and blanket structure consists of four stainless steel type 304 (SS304) shells. For the purposes of this of this exercise, only the last focusing magnet has been modeled. Figure 2 is a plot of the geometry for

the 288-beam case. Visible are the Flibe pocket with penetrations, the chamber and blankets shells, the first wall shielding packets that surround each array of beams, and the magnets themselves. The top portion of the geometry has been removed to allow one to see inside the chamber. Similar models have been used for the 72-, 128-, and 200-beam cases. Neutron and γ -ray transport calculations have been completed using the TART98 Monte Carlo code [7]. A total of 200 million particles were transported for each case. Neutron activation calculations have been performed with the ACAB98 radionuclide generation/depletion code using the FENDL/A-2.0 activation cross section library [8,9].

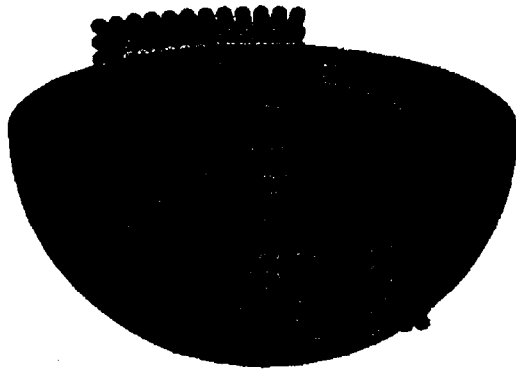


Fig. 2. View of the neutronics model for the 288-beam case.

4. Results

Results from TART98 are generated on a per-source-neutron basis. We have normalized these results according to the baseline operational parameters for the HYLIFE-II design. Specifically, we assume operation at 6.4 Hz with a target yield of 350 MJ for a total fusion power of 2240 MW [6]. Prompt heating results are presented on a per-shot basis. These results are used to determine whether or not quenching is a concern for the superconducting coils.

Cooling requirements are for steady-state operation, but they do not include radioactive afterheat from neutron activated magnet components. We assume cooling efficiencies as a function of the operational temperature: 50% for water-cooled regions, 5% for liquid-nitrogen-cooled regions, and 0.5% for liquid-helium-cooled regions. Using these efficiencies, we calculate the total recirculating power that would be needed to cool the final set of magnets. If magnet shielding is not adequate, the magnet

cooling power may represent an unacceptable loss of revenue.

Radiation damage from neutrons and γ -rays is presented for the magnet coils. These dose rates would apply to the superconducting coils, the Cu stabilizer, and any insulating materials. High dose rates may necessitate frequent maintenance and/or replacement of final focusing magnets. This may cause not only an economic penalty, but it also may be a significant source of waste [10]. Therefore, we present neutron activation results for the key major magnet subcomponents.

4.1 Magnet heating and cooling

If sufficiently high, prompt heating of the magnet coils could raise the superconducting material above its critical temperature and cause it to quench. For Nb-Ti superconductors, an energy deposition of 50-100 mJ/cc is tolerable [11]. None of the cases analyzed for this work appear to have a problem with magnet quench. Prompt heating results range from a low of 0.8 mJ/cc in the 288-beam case to a high of 1.2 mJ/cc in the 72-beam case. Given that the designs have not been optimized to reduce the heat loading on the coils, it seems unlikely that this is a serious concern. Figure 3 shows the neutron and γ -ray spectra in the magnet coils for the 72-beam case. These spectra are typical of the other cases with the γ -ray spectrum peaking at ~ 100 keV.

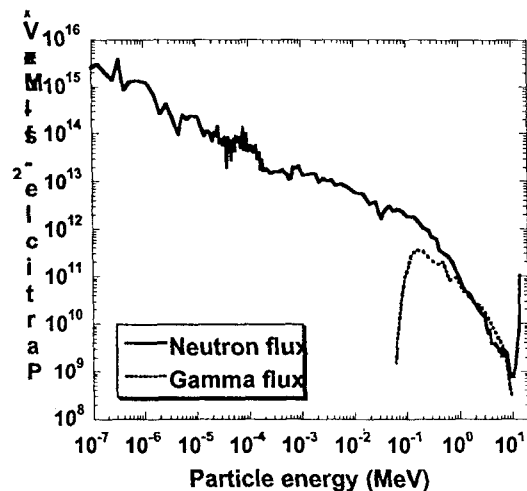


Fig. 3. Neutron and γ -ray spectra for the 72-beam case

The recirculating power that would be needed to cool the array of magnets has been calculated for each case. Our results only include the final

array of magnets, and thus, some particles that scatter from the next set of magnets have been neglected. Previous work found this to be a 10-15% effect, so we increase our results by 15% [10]. Previous work also found that the last magnet only accounted for 19-32% of the total recirculating power [10]. Using this, we estimate the total cooling power needed for all magnets and shielding material. Averaged over a magnet, γ -rays are responsible for 85-90% of the energy deposition.

The cooling powers, shown in Table 2, also include contributions from radioactive afterheat of the various magnet subcomponents (due to neutron activation and subsequent radioactive decay). In each case, afterheat is only contributes $\sim 3\%$ to the total cooling power. The cooling required due to afterheat is dominated by the tungsten shielding and the superconducting coil and stabilizer.

As indicated in the table, the recirculating power rises with the number of beams from ~ 15 MW_e for the 72-beam case up to ~ 20 MW_e for the 288-beam case. While this is certainly not negligible at $\sim 2\%$ of the electrical output of the power plant, it is for a design that has not been optimized, so it can be reduced and is probably not a significant issue.

Table 2
Magnet heating and cooling results

Parameter	Number of beams			
	72	128	200	288
Prompt heating in coils, mJ/cc	1.19	1.02	0.91	0.76
Cooling power for final quad, MW _e	3.12	3.50	4.02	4.26
Estimated* total cooling power, MW _e	11-19	13-21	14-24	15-26

* Cooling power is adjusted to correct for scattering and contributions from the other magnet arrays and auxiliary shielding materials.

4.2 Magnet dose and lifetime for base cases

The maximum dose and/or particle fluence that insulators, superconductors, and stabilizers can withstand is not certain. Data for fusion-relevant irradiations is sparse. Sawan et al. reported a lifetime dose limit of 50 MGy for epoxy electrical insulators [1]. Organic insulators are even less radiation resistant. Other work has reported a disturbing result the resistivity of copper increased by 2.5% at a neutron fluence of only 2×10^{17} n/cm² [12]. This can, of course, be

circumvented through operation at a lower current density, but this increases the radial build of the magnets, and thus, the half-angle of the beams to the target.

Hahn et al. reported that Nb₃Sn irradiated to a fluence of 2×10^{18} n/cm² showed a 3 K drop in the critical current temperature and a 2 \times reduction in the critical current density [13]. In a review paper, Sawan and Walstrom conclude that Nb-Ti can be annealed with 70% recovery after a fast neutron ($E_n \geq 0.1$ MeV) fluence of 3×10^{18} n/cm² [14]. This implies an end-of-life fluence limit of 10^{19} n/cm². They report a 20% drop in the critical current of Nb₃Sn after a fluence of 2×10^{19} n/cm² [14].

We adopt the 50 MGy value for the epoxy insulators. Additionally, we assume a total fast neutron fluence limit of 10^{19} n/cm² for the superconductors and stabilizer. This assumption needs to be validated with additional irradiations and analysis. Table 3 summarizes the dose and fast fluence results as a function of the number of beams. The magnet lifetime is estimated.

In all cases, the fast neutron fluence is the limiting factor on the magnet lifetime. Based upon a fast neutron fluence limit of 10^{19} n/cm², the magnet lifetimes range from 0.6-1.0 years. If a total dose to the magnet coils, stabilizers, and insulators of 50 MGy is the limiting factor, then the lifetimes would range from 1.3-2.0 years. In either case, the magnet lifetime is, within a factor of two, only 1 year.

Table 3
Magnet dose and lifetime for base cases

Parameter	Number of beams			
	72	128	200	288
Annual dose to coils & insulators (n + γ), MGy/y	39	33	30	25
Annual fast neutron fluence to coils & insulators, n/cm ² -y	1.7×10^{19}	1.4×10^{19}	1.3×10^{19}	1.0×10^{19}
Estimated magnet lifetime based upon annual dose & fluence, years	0.6-1.3	0.7-1.5	0.8-1.7	1.0-2.0

4.3 Neutron activation for base cases

Neutron activation calculations have been carried out using the estimated magnet lifetimes based upon a fast neutron fluence limit of 10^{19} n/cm² (lower end of the ranges shown in Table 3). In all cases, the Nb-Ti portion of the coils is

problematic in that it is a source of ^{94}Nb , a long-lived radionuclide. While a waste disposal rating (WDR) less than unity is desirable, the base cases have WDR values ranging from 6.1 for the 72-beam case to 7.7 for the 288-beam case. None of these coils would qualify for disposal via shallow land burial. The gradual increase in the WDR is primarily due to the increased lifetime for the cases with a larger number of beams. Figure 4 shows the neutron spectrum in the coils for the 72- and 288-beam cases.

Although none of the coils would qualify for disposal via shallow land burial, all appear to qualify for remote recycling. After 50 years of decay time following the irradiation, the contact dose rates range from a low of 2.9 mSv/h for the 72-beam case to 3.6 mSv/hr for the 288-beam case. Typically, remote recycling is considered possible for contact dose rates ≤ 100 mSv/h. The magnets would not qualify for hands-on recycling, however, due to its limit of only 25 $\mu\text{Sv/h}$. The contact dose rates are all dominated by ^{94}Nb , which is produced primarily at neutron energies of less than 1 eV (^{93}Nb is a classic $1/v$ absorber) and at the resonances of the $^{93}\text{Nb}(n,\gamma)^{94}\text{Nb}$ and $^{93}\text{Nb}(n,\gamma)^{94m}\text{Nb}$ reactions (0.1-1 keV). Future work may seek to reduce these reaction rates by adding materials with competing reactions in these energy ranges (e.g., boron has a large absorption cross section over both of these energy ranges).

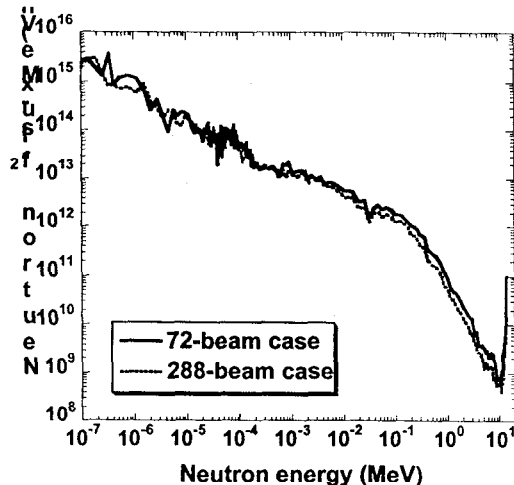


Fig. 4. Neutron spectra for the 72- and 288-beam cases

4.4 Results for enhanced case

The short estimated magnet lifetimes shown in Table 3 prompted the creation of an additional

case. While the four base case designs all included 5 cm of tungsten shielding, this shielding was increased to 10 cm for a new version of the 72-beam case. Table 4 compares the radial build and magnet properties of the enhanced, 72-beam case with the 72-beam base case. Due to the increased shielding, the outer radius of each magnet increases from 15.1 to 21.7 cm, and thus, the half-angle of the magnet array increases from 11.0 to 15.6 degrees. With the additional shielding, the array half-angle is slightly larger than that for the 200-beam base case. Recent target designs call for half-angles of 6.0 and 12.0 degrees for the foot and main pulse beams, respectively [15].

Increasing the shielding thickness from 5 to 10 cm not only pushes the inner radius of the coil out farther, but the need for a higher magnetic field results in a substantially thicker coil and banding. As a result, the coil and banding masses increase by 2.6 \times and 3.6 \times , respectively. Due to the increased masses, cooling requirements also increase relative to the 72-beam base case. The total recirculating power needed for cooling the final magnet increases from 3.1 to 3.9 MW_e , and the estimated total cooling power is 12-21 MW_e versus 11-19 MW_e for the base case. This increase is quite minor.

Table 4
Comparison of the 72-beam cases

Parameter	Shielding thickness	
	5 cm	10 cm
θ , mrad	7	7
Beam radius (max), cm	5.0	5.0
Bore radius, cm	6.8	6.8
Winding radius, cm	13.8	18.8
Banding radius, cm	14.4	20.0
Quad outer radius	15.1	21.7
Quad field, T	3.4	4.6
Field gradient, T/m	24.6	24.6
Array half-angle at target	11.0°	15.6°

The total dose rate to the coils falls by 2.2 \times from 39 MGy/y to only 18 MGy/y. The fast neutron fluence falls from 1.7×10^{19} n/cm 2 -y to 7.5×10^{18} n/cm 2 -y. Based upon these values, the magnet lifetime is estimated as 1.3-2.8 years compared with the 0.6-1.3 years for the case with only 5 cm of shielding.

The neutron activation of the magnet coil increases by about 30% due to the softened neutron spectrum. The dominant long-lived radionuclide is ^{94}Nb , which is produced predominantly via low-energy neutrons.

Nevertheless, the magnet coils would still qualify for remote recycling as the contact dose rate would be only 3.7 mSv/h at a time of 50 years after irradiation.

If we assume that increasing the shielding thickness from 5 to 10 cm would have a similar effect for the 288-beam case, then we would predict a magnet lifetime of 2.2-4.4 years. Of course, this would come with a half-angle of 26.2° for the magnet array. Such a large half-angle is incompatible with current target designs.

5. Conclusions and future work

While previous work considered drivers with only 12-20 beams and could allocate 30-40 cm of shielding per beam, recent studies push designs towards a greater number of beams to achieve substantial savings in the cost of the accelerator. Increasing the number of beams, however, leaves less room for radiation shielding, and thus, nuclear heating, radiation damage, and neutron activation may be a concern. To address this issue, we have investigated the shielding characteristics of the final focusing magnets using a self-consistent source-to-target model, which includes the final focusing parameters and only 5 cm of shielding for each magnet.

Our results indicate that the damage rate to the sensitive superconducting coils, stabilizer, and insulators falls as the number of beams is increased. This encouraging result, however, comes at the price of increased cooling power, neutron activation, and total magnet volume and mass. More importantly, the magnet array half-angles—for the cases with more than 72 beams—are incompatible with currently available target designs. Future work will need to reconcile the cost savings of using more beams with the increased final focusing cost and incompatibility with the target.

Extrapolating from our 72-beam cases, we predict a magnet lifetime of ~ 3 years for a 288-beam case with 10 cm shielding. The magnet array half-angle, however, would be more than 26°. The lifetime estimate relies heavily upon largely uncertain radiation damage limits, and thus, needs to be updated in future work. Data on neutron and γ -ray dose and fluence limits are needed for superconductors, stabilizers, and insulators.

Switching from Nb-Ti to one of the new, high- T_c superconductors such as BSCCO-2223 would greatly reduce neutron activation, however, the

radiation lifetimes are even more uncertain. Nb₃Sn results would be very similar to those presented for Nb-Ti.

It is worth noting that none of the shielding designs have been optimized for maximum performance. Given that the fast neutron fluence at the coils appears to be the limiting factor for magnet lifetime (~ 2× more restrictive than the total dose), future work will seek to minimize the fluence by modifying the shielding design to use materials with larger fast neutron cross sections. Unfortunately, this also will reduce the γ -ray shielding effectiveness of the shielding, and thus, the recirculating power and total dose to the coils likely will increase. Therefore, updated designs are likely to require an increased shielding thickness and push the target designs beyond their limits from the perspective of array half-angle. Future work must explore this trade-off between final focus shielding and target capabilities and requirements.

Acknowledgements

Work performed under the auspices of the U. S. Dept. of Energy by University of California Lawrence Livermore National Laboratory under Contract No. W-7405-Eng-48.

References

- [1] M. E. Sawan, W. F. Vogelsand, and D. K. Sze, University of Wisconsin Fusion Engineering Program Report UWFD-438 (1981).
- [2] R. F. Bourque, W. R. Meier, and M. J. Monsler, *Fusion Technol.* 21 (1992) 1465.
- [3] W. R. Meier, R. O. Bangerter, and A. Faltens, *Nuc. Inst. and Meth. A* 415 (1998) 249.
- [4] J. J. Barnard et al., *Nucl. Inst. and Meth. A* 415 (1998) 218.
- [5] R. W. Moir et al., *Fusion Technol.* 25 (1994) 5.
- [6] W. R. Meier and J. J. Barnard, this proceedings.
- [7] D. E. Cullen, Lawrence Livermore National Laboratory Report UCRL-ID-126455, Rev. 2 (1998).
- [8] J. Sanz, Universidad Nacional de Educacion a Distancia, Lawrence Livermore National Laboratory Report UCRL-CR-133040 (1999).
- [9] A.B Pashchenko et al., International Atomic Energy Agency Report IAEA-NDS-173 (1997).
- [10] J. F. Latkowski, R. W. Moir, and P. A. House, in press.
- [11] Y. Isawa, Case studies in superconducting magnets, Plenum Press, New York (1994).
- [12] R. A. von Konyenburg et al., Second topical meeting on fusion reactor materials (1981).
- [13] P. A. Hahn et al., *J. Nucl. Matl.* 179 (1991) 1127.
- [14] M. E. Sawan and P. L. Walstrom, *Fusion Technol.* 10 (Nov. 1986) 741.
- [15] D. A. Callahan-Miller and M. Tabak, *Nucl. Fusion* 39 (Jul. 1999) 883.